Fiber Optics Receiver Error Rate Prediction Using the Gram-Charlier Series

MASUD MANSURIPUR, JOSEPH W. GOODMAN, ERIC G. RAWSON, AND ROBERT E. NORTON

Abstract—**This paper applies the Gram–Charlier series method to the calculation of error probabilties in digital optical receivers. This method allows the calculation of "exact" error probabilities including the effects of avalanche noise, thermal noise, and arbitrary postdetection processing filter. The predictions of this method are compared with those of a simple Gaussian approximation and with the Chernoff bounds. Finally, the effects of modal noise are included in the theory, and some specific cases are explored numerically.**

I. INTRODUCTION

The problem of error probability calculation for a digital optical communication receiver has been considered by many authors. Rice [1] was the first to give a comprehensive treatment of this problem, although his work was not done in the context of optical communications. His results became applicable to this problem when Personick [2] studied the statistics of avalanche gain and gave a general formula for calculating its moments. However, these results are not directly suitable for error probability calculations, for they provide us with the cumulants rather than the density function itself.

Various authors [3]–[5] have applied different numerical methods to find approximations to the error probabilities of interest. Of particular importance is the work of Personick *et al.* [7], who compared various methods for calculating these probabilities. Among the methods examined was one based on the results of McIntyre [6]. This method served as the standard (or "exact" method) against which the other methods were compared.

In this paper we consider an alternative method for calculating "exact" results against which approximate methods can be compared. A Gram–Charlier expansion for the density function is used as the basis for numerical computations. A simple recursive formula for the coefficients in this expansion is presented. The ease with which the Gram–Charlier series can be integrated greatly facilitates the calculation of error probabilities.

Section II contains a brief sketch of the theoretical framework underlying the calculations. Section III contains numerical results for both "biphase" and "integrate and dump" receivers. Of special interest is the comparison of the predictions based on the Gram–Charlier series with the predictions based on a Gaussian approximation [7] and predictions based on the Chernoff bound [2], [7]. Section IV contains new results that allow the prediction of the effects of "modal noise" on error probability, again by means of a Gram–Charlier expansion. Section V contains concluding remarks, and the Appendix contains the theoretical background for the calculations of Section IV.

Paper approved by the Editor for Transmission Systems of the IEEE Communications Society for publication without oral presentation. Manuscript received March 13, 1979; revised August 8, 1979.

M. Mansuripur and J. W. Goodman are with the Department of Electrical Engineering, Stanford University, Stanford, CA 94305.

E. G. Rawson and R. E. Norton are with the Xerox Palo Alto Research Center, Palo Alto, CA 94304.

II. THEORY

A model for a direct detection optical receiver that uses an avalanche photodiode is shown in Fig. 1. It is known [1], [7] that the characteristic function of the random voltage at the decision point is given by

$$\psi(S) = \exp\left(\sum_{n=1}^{\infty} \frac{\lambda_n S^n}{n!}\right) \tag{1}$$

where λ_n is the nth cumulant of the distribution and is given by

$$\lambda_n = (\eta/h\nu)(qRA)^n\langle G^n\rangle \int_0^T \hat{P}(\tau)h^n(T-\tau)\,d\tau. \tag{2}$$

Here the symbols have the following meanings:

- η is the quantum efficiency
- h is Planck's constant,
- ν is the optical frequency,
- q is the charge of an electron,
- R is the input resistance of the postdetection amplifier,
- A is the amplifier gain,
- $\langle G^n\rangle$ is the nth moment of avalanche gain,
- T is the duration of the waveform representing a single bit,
- $\hat{P}(\tau)$ represents the time-varying optical power incident on the photodetector, and
- $h(\tau)$ is the impulse response of the linear and time-invariant signal-processing filter.

This characteristic function $\psi(S)$ is derived under the assumption that for each bit, $\hat{P}(\tau)$ is a known, deterministic function and that the photodetection process (before avalanche gain) obeys Poisson statistics. The effect of random avalanche gain is taken into account through the moments $\langle G^n\rangle$, which can be calculated from the following recursive relation [2], [4]:

$$\langle G^n\rangle = \sum_{m=1}^{2n-1} C_{n,m}\langle G\rangle^m \tag{3}$$

where

$$\begin{aligned} C_{n+1,m} &= -m(1-k)C_{n,m} + [1+(m-1)(1-2k)] \\ &\quad \cdot C_{n,m-1} + (m-2)kC_{n,m-2} \\ C_{n,m} &= 0 \qquad \text{if } m \leqslant 0 \qquad \text{or } m \geqslant 2n. \\ C_{1,1} &= 1 \end{aligned} \tag{4}$$

Here k is the ionization ratio of the avalanche diode and $\langle G\rangle$ is its average gain.

The effect of thermal noise of variance σ_{th}^2 at the decision point is taken into account by replacing λ_2 by $\lambda_2 + \sigma_{th}^2$, the reason being that the characteristic function of Gaussian thermal noise is $\exp(\sigma_{th}^2 S^2/2!)$. Since it is independent of other noise processes, its characteristic function must multiply the characteristic function $\psi(S)$ in (1).

For computational purposes, it is often convenient to normalize the random variable at the decision point so that

0090-6778/80/0300-0402$00.75

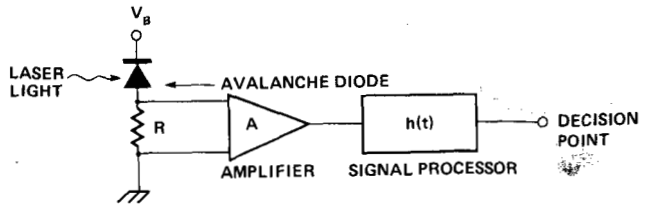

Fig. 1. Schematic of receiver model.

it has zero mean and unit variance. Such normalization changes the cumulants λ_n to $\tilde{\lambda}_n$ as follows:

$$\tilde{\lambda}_1 = 0 \quad \tilde{\lambda}_n = \frac{\lambda_n}{\lambda_2^{n/2}} \qquad n \geqslant 2. \tag{5}$$

One way to obtain the density function of a random variable from knowledge of its cumulants is to use the Gram-Charlier series expansion of the density function, namely,

$$p(x) = \sum_{n=0}^{\infty} a_n \varphi_n(x)$$

where

$$\varphi_n(x) = \frac{d^n}{dx^n}\left[\frac{1}{\sqrt{2\pi}} \exp(-x^2/2)\right]. \tag{6}$$

The corresponding characteristic function of $p(x)$ is

$$\begin{aligned}\psi(S) &= \int_{-\infty}^{+\infty} \exp(Sx) p(x)\, dx \\ &= \sum_{n=0}^{\infty} a_n \int_{-\infty}^{+\infty} \exp(Sx) \frac{d^n}{dx^n}\left[\frac{1}{\sqrt{2\pi}} \exp(-x^2/2)\right] dx \\ &= \sum_{n=0}^{\infty} (-1)^n a_n S^n e^{S^2/2} = \left[\sum_{n=0}^{\infty} \mu_n \frac{S^n}{n!}\right] \exp(S^2/2)\end{aligned} \tag{7}$$

where

$$\mu_n = (-1)^n \cdot n! \cdot a_n. \tag{8}$$

On the other hand, for the normalized random variable, the characteristic function is also given by

$$\psi(S) = \exp\left\{\sum_{n=1}^{\infty} \tilde{\lambda}_n S^n/n!\right\}. \tag{9}$$

Since $\tilde{\lambda}_1 = 0$ and $\tilde{\lambda}_2 = 1$, we find

$$\sum_{n=0}^{\infty} \mu_n \frac{S^n}{n!} = \exp\left\{\sum_{n=3}^{\infty} \tilde{\lambda}_n S^n/n!\right\}. \tag{10}$$

Using the recursive relationship between central moments and cumulants [4], it can be shown that

$$\mu_0 = 1$$

$$\mu_1 = \mu_2 = 0$$

$$\mu_3 = \tilde{\lambda}_3$$

$$\mu_{n+1} = \tilde{\lambda}_{n+1} + \sum_{m=2}^{n-1} \binom{n}{m} \tilde{\lambda}_{m+1} \mu_{n-m}, \qquad n \geqslant 3. \tag{11}$$

Therefore, the coefficients a_n in the Gram-Charlier series expansion can be computed from (11) and (8). Noting the recursion relation

$$\varphi_n(x) = -\{x\varphi_{n-1}(x) + (n-1)\varphi_{n-2}(x)\} \tag{12}$$

where

$$\varphi_0(x) = \frac{1}{\sqrt{2\pi}} \exp(-x^2/2)$$

and

$$\varphi_1(x) = -\frac{x}{\sqrt{2\pi}} \exp(-x^2/2),$$

we see that the probability density function $p(x)$ could easily be calculated with a digital computer, provided the Gram-Charlier series is truncated after a certain number of terms.

What we really wish to know is the cumulative probability distribution function of the random variable x from which error probabilities can be calculated. The desired probabilities are obtained from the relationships

$$\int_{-\infty}^{x_0} p(x)\, dx = \tfrac{1}{2}(1 - \operatorname{erf}(-x_0/\sqrt{2})) + \sum_{n=3}^{\infty} a_n \varphi_{n-1}(x_0),$$

$$(x_0) \leqslant 0$$

$$\int_{x_0}^{+\infty} p(x)\, dx = \tfrac{1}{2}(1 - \operatorname{erf}(x_0/\sqrt{2})) - \sum_{n=3}^{\infty} a_n \varphi_{n-1}(x_0), \qquad x_0 \geqslant 0 \tag{13}$$

where

$$\operatorname{erf}(x_0) = \frac{2}{\sqrt{\pi}} \int_0^{x_0} e^{-x^2/2}\, dx. \tag{14}$$

III. NUMERICAL RESULTS

Two basic signaling schemes are considered here. In the first, a binary 1 is represented by a rectangular pulse of power P_0, while a binary 0 is represented by a rectangular pulse of power $(1 - m)P_0$. The parameter m is referred to as the "modulation depth." The signal processing filter used in this case has a rectangular impulse response with a duration equal to that of a signal pulse. We refer to this particular method of signaling and detection as "integrate and dump." Fig. 2 shows the transmitted waveforms and the impulse response of the signal processing filter.

The second signaling method, illustrated in Fig. 3, is referred to as "biphase" signaling. Here a binary 1 is represented by a down-stepping pulse, while a binary 0 is represented by

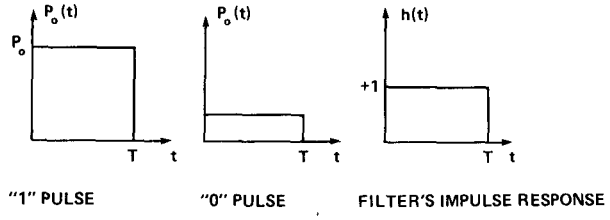

Fig. 2. Signals and filter impulse response in the integrate-and-dump detection case.

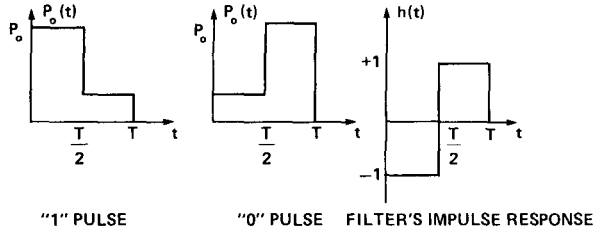

Fig. 3. Signals and filter impulse response in the biphase detection case.

an "up-stepping" pulse. The signal processing filter is taken to have an impulse response that is a negative rectangular pulse followed by a positive rectangular pulse.

The Gram–Charlier method described in the previous section is now used to calculate error probabilities in several cases of interest. These results are compared with those of two other methods for predicting error probabilities, one based on the approximation that the voltage at the decision point obeys Gaussian statistics (taking account of the effect of avalanche gain on the first and second moments), and the second based on the Chernoff bound method [2], [7]. The number of terms used in the Gram–Charlier series varied from 4 to 50, depending on the rapidity of convergence. The computing time required for the Gram–Charlier series was greater than that required for the Chernoff bound, but the former method is more accurate than the latter by an order of magnitude, as the results will show. For simplicity, the Gram–Charlier series solution is hereafter referred to as the "exact" solution, it being understood that for any specific numerical results presented, the number of terms used in the series was chosen to be large enough to allow verification of convergence.

The optical system parameters assumed for these calculations are listed in Table I. Results for the integrate-and-dump receiver will be represented graphically with broken lines, while for the biphase receiver they will be represented by solid lines. In all cases, the detector threshold is chosen to make the false-alarm and miss probabilities equal to each other.

Fig. 4 shows plots of the predicted error probabilities P_e versus avalanche gain $\langle G \rangle$ for three methods of calculation and for both methods of signaling. The following observations can be drawn from these curves.

1) All three methods of calculation predict an error probability that initially falls with increasing $\langle G \rangle$, levels out, and finally increases with increasing $\langle G \rangle$. For the parameter values of Table I, the exact solution suggests that the optimum gain is about 140.

2) The two signaling methods have identical performances as predicted by the exact method, and the Chernoff bounds are the same for both. However, the Gaussian approximation predicts different performances for the two methods.

TABLE I
PARAMETERS USED IN THE NUMERICAL CALCULATIONS

Parameter	Definition	Numerical Value
η	Quantum efficiency	0.85
ν	Frequency of light	3.5×10^{14} Hz
R	Input resistance	1 Ω
A	Amplifier gain	1
k	Ionization ratio for the APD	0.02
T	Pulse duration	10^{-8} s
$(\sigma_{th}/q)^2$	Thermal noise variance normalized to electron charge	10^7
m	Modulation depth	0.75

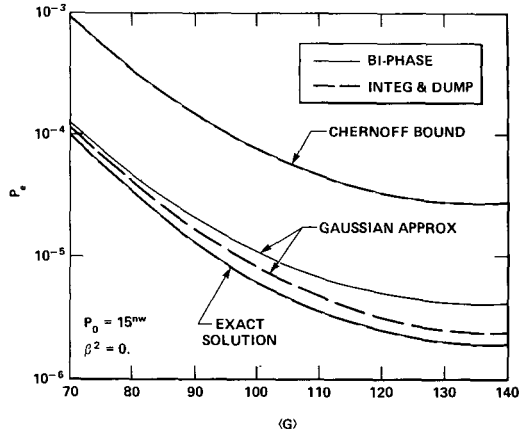

Fig. 4. Error probability versus avalanche gain as predicted by different methods and for different detection schemes.

3) The Gaussian approximation is best at low gains and worst at high gains. Its predictions are more accurate for the integrate-and-dump receiver than for the biphase receiver. In all cases considered here, the Gaussian approximation overestimates the error probability, but its predictions were always within a factor of 3 of the exact results.

4) The Chernoff bounds overestimate the error probabilities by about a factor of ten at low gains and somewhat more at high gains.

Fig. 5 shows a plot of the error probability P_e versus the optical power P_0 falling on the detector when an optimum gain is used. Only the biphase receiver is considered, and only the Gaussian approximation and the exact solutions are shown. The Gaussian approximation is again found to be accurate to within a factor of 3 over a wide range of error probabilities.

IV. EFFECTS OF MODAL NOISE

When the optical source is highly coherent, an optical communication system can suffer from an additional noise that arises within the fiber itself. This type of noise is referred to as "modal noise" [8], [9], and arises from micromotion of the fiber together with the resulting differential phase delays introduced in the various propagating modes. Alternatively, such noise can also arise in a perfectly stationary fiber if the frequency of the optical source changes due to thermal or other effects.

If the coherence time of the light radiated by the source is longer than the time delay difference suffered by the various propagating modes, then those modes interfere to form a speckle pattern at the end of the fiber. This speckle pattern changes in time with micromotion of the fiber or with suf-

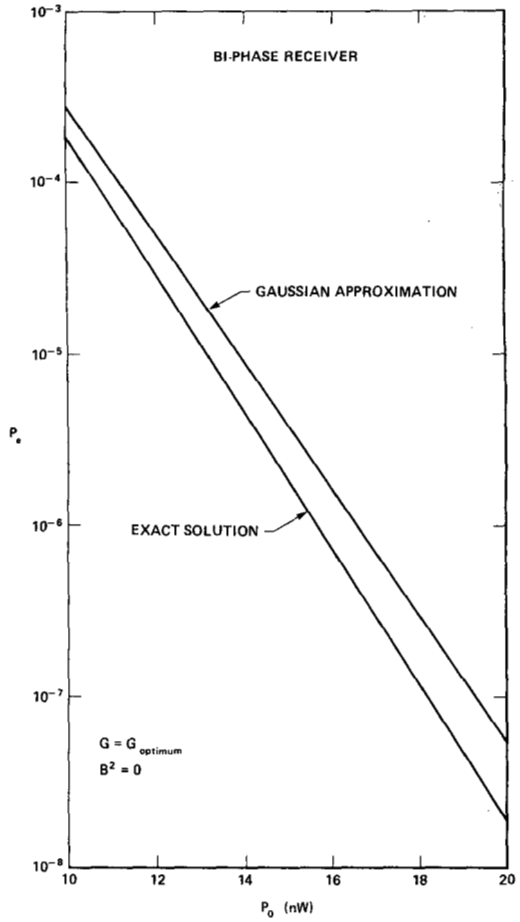

Fig. 5. Error probability versus input power to the detector for bi-phase detection scheme. Each point on the curve is calculated at the corresponding optimum gain.

ficiently large frequency shifts of the light. If this fiber is partially coupled to one or more other fibers, either by means of a power splitter or with a somewhat misaligned joint connector, fluctuations of the transmitted light power will be observed as the moving speckle pattern is only partially intercepted by the fiber that follows. Such fluctuations can degrade the error probabilities achieved by the optical communication system. Our purpose here is to predict the effects of such noise on these error probabilities.

The average area of an individual speckle is known to approximately equal the ratio of the square of the wavelength λ to the solid angle Ω subtended by the optical rays converging towards a point in the speckle pattern [10]:

$$A_s = \frac{\lambda^2}{\Omega}. \tag{15}$$

If the speckle pattern falls on an area A of the end of the second fiber, then the average number of speckles intercepted by the latter fiber is

$$M = \frac{A}{A_s} = \frac{A\Omega}{\lambda^2}. \tag{16}$$

If the two fibers have different numerical apertures, then the smaller numerical aperture must be used to determine Ω. We have also made the implicit assumption that the numerical apertures are constant across the cores of the fibers, as would be true for step-index fibers.

If the illuminated area A on the second fiber represents only a part of the total speckle pattern, then shifts of the speckles result in random fluctuations of the amount of transmitted power. It is known [10] that for fully developed speckle, the statistics of the power transmitted by a finite aperture of area A are described by a gamma distribution with parameter M given by (16). If M is much larger than unity, the gamma distribution is well approximated by a Gaussian distribution. Thus, the fraction of the power transferred from the first fiber to the second fiber is approximately a Gaussian random variable, with a ratio of standard deviation to mean given by

$$\beta = \frac{\sigma_P}{P} = \frac{1}{\sqrt{M}}. \tag{17}$$

As might be expected, the severity of the power fluctuations depends entirely on the average number of speckles that carry power into the second fiber.

Let the power incident on the optical detector at the end of the second fiber be written

$$P(t) = \hat{P}(t) + N(t) \tag{18}$$

where $\hat{P}(t)$ is the average power, while $N(t)$ corresponds to the speckle-induced fluctuations. In the most general case, $N(t)$ can be taken to be a Gaussian random process with autocorrelation function

$$R_N(t, s) = \langle N(t)N(s)\rangle. \tag{19}$$

It is shown in the Appendix that the characteristic function of the voltage at the receiver decision point becomes

$$\psi(S) = \exp\left(\sum_{n=1}^{\infty} \Lambda_n S^n/n!\right) \tag{20}$$

where the cumulants are given by

$$\begin{aligned}\Lambda_n = {} & (\eta/h\nu)(qRA)^n \langle G^n\rangle \int_0^T \hat{P}(\tau)h^n(T-\tau)\,d\tau \\ & + \tfrac{1}{2}(\eta/h\nu)^2(qRA)^n \sum_{m=1}^{n-1}\binom{n}{m}\langle G^m\rangle\langle G^{n-m}\rangle \\ & \cdot \int_0^T\int_0^T R_N(t, s)h^m(T-t)h^{n-m}(T-s)\,dt\,ds. \end{aligned} \tag{21}$$

For the case of modal noise, the fluctuations of power occur at a much slower rate than the bit rate of the system. Thus, during any single bit decision period, the modal noise can be taken to be approximately constant (but still a random value). With this assumption, the autocorrelation function of the noise fluctuations takes the form

$$R_N(t, s) = \beta^2\hat{P}(t)\hat{P}(s) \tag{22}$$

and (21) becomes

$$\Lambda_n = (\eta/h\nu)(qRA)^n\langle G^n\rangle \int_0^T \hat{P}(\tau)h^n(T-\tau)\,d\tau + \frac{\beta^2}{2}\sum_{m=1}^{n-1}\binom{n}{m}\left[(\eta/h\nu)(qRA)^m\langle G^m\rangle \cdot \int_0^T \hat{P}(\tau)h^m(T-\tau)\,d\tau\right] \times \left[(\eta/h\nu)(qRA)^{n-m}\langle G^{n-m}\rangle \cdot \int_0^T \hat{P}(\tau)h^{n-m}(T-\tau)\,d\tau\right]. \quad (23)$$

Reference to (2) shows that the cumulants Λ_n in the presence of modal noise are related to the cumulants λ_n in the absence of modal noise by

$$\Lambda_n = \lambda_n + \beta^2 \sum_{m=1}^{n-1} \frac{1}{2}\binom{n}{m}\lambda_m\lambda_{n-m}. \quad (24)$$

Note that when the modal noise parameter β^2 approaches zero, the two sets of cumulants become indistinguishable.

It is now possible to apply the Gram–Charlier method to find the error probabilities achieved for various values of β^2. Fig. 6 shows the resulting variation of error probability P_e with avalanche gain $\langle G\rangle$ for a biphase receiver. The curve for $\beta^2 = 0$ corresponds to the case of no modal noise present. The curves for $\beta^2 = 0.005$ and 0.02 correspond to situations in which the average number of speckles intercepted by the second fiber are 200 and 50, respectively. Considering that a 100 μm diameter fiber with a numerical aperture of 0.3 used with light of wavelength 1 μm produces about 2500 speckles across its end, it can be seen that rather severe misalignments would be necessary to seriously affect the error probabilities for such a fiber. For smaller fibers with smaller numerical apertures, the phenomenon poses a more severe problem.

The point of this discussion in this section has been simply to demonstrate that the Gram–Charlier method can be fruitfully applied to other statistical analysis problems encountered in optical communications. The method has been found to yield satisfactorily convergent series for most cases of practical interest, and to be reasonably efficient from a computational point of view.

CONCLUDING REMARKS

The Gram–Charlier series has proved to be a useful tool in analyzing the "exact" error probabilities for various types of optical communication systems. The analysis has taken full account of both avalanche noise and thermal noise. The Chernoff-bound method of estimating error probabilities has been found to yield predictions that are at least a factor of ten too pessimistic for the particular system parameters used here. The use of a Gaussian approximation for the detector statistics yields much more accurate results, but the quality of this approximation depends somewhat on the signal waveforms chosen to represent binary ones and zeros and the particular postdetection filter that is used. Finally, the Gram–Charlier-series method has been successfully applied to the problem of determining error probabilities in the presence of modal noise.

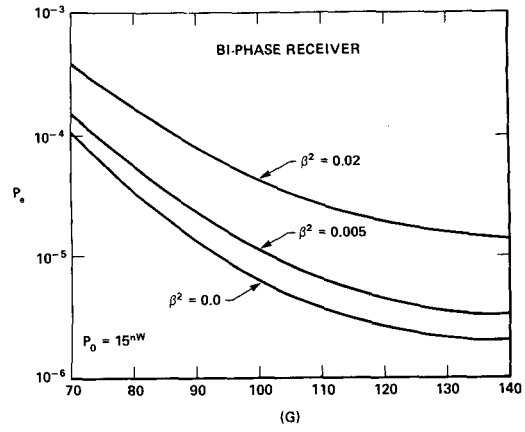

Fig. 6. Error probability versus avalanche gain in the presence of speckles.

APPENDIX

INCLUSION OF THE INPUT NOISE IN THE GENERAL CHARACTERISTIC FUNCTION

The conditional characteristic function of the random variable at the decision point given the input power $P(\tau)$ is

$$\psi_c(S) = \exp\left\{\sum_{n=1}^{\infty} \lambda_n S^n/n!\right\} \quad (A1)$$

where

$$\lambda_n = (\eta/h\nu)(qRA)^n\langle G^n\rangle \int_0^T P(\tau)h^n(T-\tau)\,d\tau. \quad (A2)$$

If $P(\tau) = \hat{P}(\tau) + N(\tau)$, where $\hat{P}(\tau)$ is the average input power and $N(\tau)$ is a zero-mean random process, then the general characteristic function will be the expectation of $\psi_c(S)$ over the ensemble of all sample functions $N(\tau)$. From (A2) we have

$$\lambda_n = \hat{\lambda}_n + (\eta/h\nu)(qRA)^n\langle G^n\rangle \int_0^T N(\tau)h^n(T-\tau)\,d\tau \doteq \hat{\lambda}_n + \sum_{j=1}^{J} N(\tau_j)\cdot\{(\eta/h\nu)(qRA)^n\langle G^n\rangle h^n(T-\tau_j)\Delta\tau_j\} = \hat{\lambda}_n + N_J{}^T \cdot H_{n,j} \quad (A3)$$

where N_J is a $J \times 1$ column vector whose jth element is $N(\tau_j)$ and $H_{n,J}$ is another $J \times 1$ column vector whose jth element is $(\eta/h\nu)(qRA)^n < G^n > h^n(T-\tau_j)\Delta\tau_j$. Therefore,

$$\psi_c(S) = \exp\left\{\sum_{n=1}^{\infty} \hat{\lambda}_n S^n/n!\right\} \cdot \exp\{N_J{}^T \cdot H_J(S)\} \quad (A4)$$

where

$$H_J(S) = \sum_{n=1}^{\infty} H_{n,J} \cdot \frac{S^n}{n!}. \tag{A5}$$

Now if the assumption is made that N_J is a Gaussian vector with $E[N_J \cdot N_J{}^T] = R$ we can write

$$\begin{aligned}\psi(S) &\doteq \int_{-\infty}^{+\infty} \cdots \int_{-\infty}^{+\infty} \psi_c(S) \cdot \frac{1}{(2\pi)^{J/2} \cdot \| R \|^{1/2}} \\ &\quad \cdot \exp\{-\tfrac{1}{2} N_J{}^T R^{-1} N_J\}\, dN_J \\ &= \exp\left\{ \sum_{n=1}^{\infty} \hat{\lambda}_n \frac{S^n}{n!} + \tfrac{1}{2} H_J{}^T(S) \cdot R \cdot H_J(S) \right\} \\ &= \exp\left\{ \sum_{n=1}^{\infty} \hat{\lambda}_n \frac{S^n}{n!} + \frac{1}{2} \sum_{k=1}^{\infty} \sum_{l=1}^{\infty} H_{k,J}{}^T \cdot R \cdot H_{l,j} \frac{S^{k+l}}{k!l!} \right\}.\end{aligned} \tag{A6}$$

In the limit when the partition becomes infinitely fine, $\psi(S)$ will be given by

$$\begin{aligned}\psi(S) = \Bigg\{ \exp \sum_{n=1}^{\infty} \hat{\lambda}_n \frac{S^n}{n!} + \frac{1}{2} \sum_{k=1}^{\infty} \sum_{l=1}^{\infty} \Bigg[& (\eta/h\nu)^2 (qRA)^{k+l} \\ & \cdot \langle G^k \rangle \cdot \langle G^l \rangle \int_0^T \int_0^T R(t, s) h^k (T-t) h^l \\ & \cdot (T-s)\, dt\, ds \Bigg] \frac{S^{k+l}}{k!l!} \Bigg\},\end{aligned} \tag{A7}$$

which can be written in the following more compact form:

$$\psi(S) = \exp\left\{ \sum_{n=1}^{\infty} \Lambda_n \frac{S^n}{n!} \right\} \tag{A8}$$

where

$$\begin{aligned}\Lambda_1 &= \hat{\lambda}_1 \\ \Lambda_n &= \hat{\lambda}_n + \sum_{m=1}^{n-1} \frac{1}{2} \binom{n}{m} (\eta/h\nu)^2 (qRA)^n \langle G^m \rangle \\ &\quad \cdot \langle G^{n-m} \rangle \cdot \int_0^T \int_0^T R(t, s) h^m (T-t) h^{n-m} \\ &\quad \cdot (T-s)\, dt\, ds \qquad n \geqslant 2,\end{aligned} \tag{A9}$$

REFERENCES

[1] S. O. Rice, "Mathematical analysis of random noise," *Bell Syst. Tech. J.*, vol. 23, 1944.

[2] S. D. Personick, "Statistics of a general class of avalanche detectors," *Bell Syst. Tech. J.*, vol. 50, pp. 3075–3095, Dec. 1971.

[3] W. Hauk, F. Bross, and M. Ottka, "The calculation of error rates for optical fiber systems," *IEEE Trans. Commun.*, vol. COM-26, July 1978.

[4] R. Dogliotti, A. Luvison, and G. Pirani, "Error probabiltiy in optical fiber transmission systems," *IEEE Trans. Inform. Theory*, vol. IT-25, Mar. 1979.

[5] G. Cariolaro, "Error probability in digital fiber optic communication systems," *IEEE Trans. Inform. Theory*, vol. IT-24, Mar. 1978. This reference uses the Gram–Charlier series to predict the error probabilities in an optical communication system. However, the emphasis is on intersymbol interference, and an approximation equivalent to the simple Gaussian approximation of our Section III is made. Thus, the problem solved is a different one from the problem solved here.

[6] R. J. McIntyre, "The distribution of gain in uniformly multiplying avalanche diodes," *IEEE Trans. Electron Devices*, vol. ED-19, June 1972.

[7] S. D. Personick, P. Balaban, J. H. Bobsin, and P. R. Kumar, "A detailed comparison of our approaches to the calculation of the sensitivity of optical fiber system receivers," *IEEE Trans. Commun.*, vol. COM-25, pp. 541–548, May 1977.

[8] R. E. Epworth, "The phenomenon of modal noise in analogue and digital optical fibre systems," in *Proc. 4th European Conf. on Optical Commun. (4th ECOC)*, Geneva, Switzerland, Sept. 12–15, 1978.

[9] ——, "Phenomenon of modal noise in fiber systems," in *Tech. Dig. of Topical Meeting on Optical Fibre Commun.*, Washington, DC, Mar. 6–8, 1979.

[10] J. W. Goodman, "Statistical properties of laser speckle patterns," in *Laser Speckle and Related Phenomena*, J. C. Dainty, Ed. Heidelberg: Springer-Verlag, 1975.